Biophysical Journal Volume 96 March 2009 2405–2414

Quantifying Cell-Surface Biomarker Expression in Thick Tissues with Ratiometric Three-Dimensional Microscopy

Jonathan T. C. Liu,[†‡*] Mike W. Helms,[‡] Michael J. Mandella,[†] James M. Crawford,[§] Gordon S. Kino,[†] and Christopher H. Contag[‡]

[†]Ginzton Labs, Department of Electrical Engineering, Stanford University, and [‡]Clark Center for Biomedical Engineering and Sciences, Stanford University School of Medicine, Stanford, California; and [§]Department of Pathology, Immunology and Laboratory Medicine, University of Florida College of Medicine, Gainesville, Florida

ABSTRACT The burgeoning fields of in vivo three-dimensional (3D) microscopy and endomicroscopy, as well as ex vivo tissue cytometry have introduced new challenges for tissue preparation and staining with exogenous molecular contrast agents. These challenges include effective delivery of the agents, and once delivered, distinguishing between bound verses unbound molecular probes. If applied topically, there are additional issues with rinsing off unbound probe, which can be nonuniform and inefficient in thick tissues, thus leading to ambiguous contrast and a large nonspecific background that may obscure molecule-specific staining. Therefore, we have developed a ratiometric 3D microscopy scheme that not only reduces the effects of nonspecific sources of contrast, but also enables quantification of the relative binding affinity of imaging probes to their biomarker targets. Here we demonstrate this ratiometric approach by simultaneously imaging a HER2/neu (erbB2)-targeted monoclonal antibody labeled with one fluorophore and an isotype-matched negative control antibody labeled with another fluorophore. By taking a pixel-by-pixel calibrated ratio between the signals from each fluorescent image channel, accurate quantification of specific versus nonspecific binding affinity is achieved with cultured cells, yielding data that are in agreement with analyses via flow cytometry. We also demonstrate quantitative 3D microscopic imaging of biomarker expression in tissue models and in thick human biopsy samples of normal, HER2-negative, and HER2-positive breast tumors. This strategy enables rapid, quantitative, and unambiguous volumetric microscopy of biomarker expression in thick tissues, including whole biopsies, and will enable real-time optical assessment of disease markers in the living body.

INTRODUCTION

Significant and rapid advances are being made in in vivo microscopy, as seen for example by the recent development of endomicroscopes that allow for noninvasive optical sectioning and real-time microscopic analyses of living tissues (1–9). These technologies offer the promise of real-time imaging of glandular and cellular morphology, beneath the epithelial or mucosal surface, without having to cut the tissue. Such advances will provide guidance for tissue sampling, leading to more informed biopsies, and perhaps the replacement of some biopsies with noninvasive imaging, or ''optical biopsies''. Many of these approaches have relied upon intrinsic contrast between diseased versus normal tissues. Although useful in some cases, these differences are often subtle and uninformative. The use of contrast agents that target specific molecular biomarkers is a hallmark of immunohistochemistry. If vital immunolabeling can be made possible in vivo, it would enable earlier disease detection and more accurate diagnosis and staging of disease.

The use of exogenous contrast agents for three-dimensional (3D) microscopy of fresh intact tissues presents unique challenges that cannot be addressed by methods for conventional immunohistochemical analysis. Cellular and molecular studies of excised tissues rely upon exacting specimen preparation, including tissue fixation, embedding, physical sectioning, mounting on slides, staining, and rinsing before molecular interrogation. When using antibodies that target specific disease markers in conventional immunohistochemistry, elaborate blocking and rinsing protocols have been developed to minimize background staining and to reduce erroneous sources of contrast. Such protocols are not possible in thick or live tissues due to poor access to cells deep in the tissues, limited ability to wash off unbound probe, and severe time constraints for the acquisition of relevant data. Since the application of exogenous contrast agents, as well as the rinsing away of unbound probe, is neither efficient nor uniform in fresh intact tissues, a large nonspecific background often exists, along with nonspecific sources of contrast that are unrelated to the molecular target(s) of interest.

Molecularly targeted in vivo microscopy in humans has recently been demonstrated (8). Confocal endomicroscopic imaging revealed that a topically applied heptapeptide, conjugated to fluorescein dye, demonstrated preferential binding to areas of dysplasia in the human colon. In a related study, the same confocal endomicroscope was used to image fluorescence contrast from an untargeted sodium fluorescien dye (9). This second study concluded that morphological or physiological alterations in dysplastic foci leads to enhanced retention of the untargeted dye as compared to normal colonic

Submitted November 3, 2008, and accepted for publication December 15, 2008.

*Correspondence: jonliu@stanfordalumni.org

Editor: Alberto Diaspro.

0006-3495/09/03/2405/10 $2.00

doi: 10.1016/j.bpj.2008.12.3908

mucosa, demonstrating the potential of using this dye as a diagnostic stain. Since the second study (9) indicated that the accumulation of contrast agents can be significant owing to anatomical and physiological changes alone, without molecular targeting, the first study of specific molecular binding (8) would have benefited from a technique that could remove such confounding nonspecific effects. In general, possible sources of nonspecific contrast include: nonuniform application and transport kinetics of molecular probes, nonuniform application and kinetics of the rinsing medium, poor optical contact between the microscope and tissue, and the accumulation or pooling of contrast agents due to uneven tissue geometry or morphology. A method to remove, or otherwise manage these nonspecific sources of contrast during real-time 3D microscopy is needed.

With in vivo microscopy, the ability to quantify binding affinity is particularly important due to the small fields of view that are imaged. In macroscopic imaging approaches, one is often able to image both diseased and adjacent normal tissues within the same field of view, thereby providing a convenient reference for comparison. Within a microscopic field of view, however, it is difficult to image the exact transition between tissue types. This can be addressed by stitching together many fields of view into a mosaic, but this still does not provide an absolute measure of binding affinity that accounts for nonspecific contrast.

Ratiometric imaging has previously been used to improve the sensitivity and to quantify fluorescence microscopic detection of Ca^{2+}-sensitive dyes (10,11), pH-sensitive dyes (12), and FRET (fluorescence resonance energy transfer) reporters using bench top microscopes (13,14). In wide-field fluorescence imaging of an exogenous contrast agent, a double ratio technique has been developed to eliminate the effects of autofluorescence and tissue scattering variations for improved quantification of probe concentration (15,16). However, the double ratio technique does not distinguish between molecularly targeted versus nonspecific probe accumulation in tissues, which is likely to be a major challenge for interpretation of images obtained in vivo. Advances in ratiometric imaging and the application of this method to miniature clinical microscopes will both improve our ability to rapidly analyze thick tissues such as intact biopsies (''tissue cytometry'' or ''tissomics'') (17,18), as well as to analyze tissues that still reside in patients.

To address the significant challenges of in vivo microscopy and analysis of thick tissues, we have developed a method that both reduces the effects of nonspecific sources of contrast and provides a quantitative map of the binding affinity of targeted molecular probes for their intended biomarker. The technique we have developed utilizes a two-color optical-sectioning microscope for simultaneous imaging of a targeted imaging probe, at one wavelength, with an appropriate negative control at the second wavelength. By imaging a calibrated ratio of the signals from both of these channels, we demonstrate accurate quantification of biomarker expression and effective suppression of nonspecific signals and background. This technique may be generalized to a variety of molecular targeting mechanisms, as well as a variety of scanning 3D optical sectioning technologies, such as confocal microscopy and two-photon microscopy. The method is demonstrated here using the well-characterized HER2/neu (erbB2) monoclonal antibody (aka Herceptin) as the molecular targeting moiety. This antibody targets a receptor tyrosine kinase that is overexpressed in ~20–30% of human breast cancers. A nonspecific monoclonal antibody of the same isotype as the HER2/neu (erbB2) antibody was used in a manner similar to its use in flow cytometry as a control for nonspecific staining. To obtain 3D microscopic data sets in this study, we used a dual-axis confocal microscope designed by our group for deep tissue imaging. To our knowledge, this is the first demonstration of a two-color ratiometric technique to quantify the level of specific binding of an exogenous fluorophore, and to reduce the effects of nonspecific probe accumulation, for improved detection of a molecular biomarker with in vivo and ex vivo 3D microscopy of thick tissues.

METHODS

Cells and cell culture

Three breast cancer cell lines were used for quantitative ratiometric microscopy, as well as for flow cytometry validations. The SKBR3 cell line (purchased from ATCC, Manassas, VA) was used as a strong positive control for HER2/neu expression. In addition, MDA-MB-468 breast cancer cells, transfected to express a weaker and variable level of HER2/neu, were used for quantitative imaging (MDA-HER2) (19). A mock-transfected version of the same cell line (MDA-NEO) was used as a negative control.

SKBR3 cells were grown in McCoy's 5A medium supplemented with 10% fetal bovine serum and 1% penicillin/streptomycin at 37°C in a 5% CO_2 incubator. MDA-HER2 and MDA-NEO cells were grown in Dulbecco's modified Eagle's medium supplemented with 5% fetal bovine serum and 1% penicillin/streptomycin. At 75% confluence, the medium was aspirated and the cells were detached with 1.5 mL 0.05% trypsin-EDTA. After neutralization, the cells were pelleted at 300 $\times$ g for 5 min. The pellet was resuspended in 100 μL PBS per 1 $\times$ 10^6 cells.

Antibodies and fluorescence labeling

An anti-HER2/neu monoclonal antibody (mAb), without BSA and Azide, was obtained from Thermo Scientific (Waltham, MA, catalog No. MS-229-PABX). This mAb (clone 9G6.10) was labeled with LI-COR (Lincoln, NE) IRDye 800CW *N*-hydroxysuccinimide ester according to manufacturer's recommendations that were provided with a microscale protein labeling kit from LI-COR (928-38044). In summary, 20 μg of IRDye 800CW *N-H*ydroxysuccinimide ester was reacted for 2 h with 100 μg of mAb in a 115-μL volume of 1$\times$ phosphate buffered saline (PBS) (pH 8.5). A Pierce Zeba Desalting Spin column (Rockford, IL) was used for purification. The final yield was ~90% with an average labeling ratio of ~six dye molecules per antibody molecule.

An isotype-matched control mAb (Mouse IgG1), labeled with Alexa Fluor 647, was obtained from eBioscience (51-4714) (San Diego, CA). The average dye labeling ratio of this product (lot No. E023666) was reported by the manufacturer to be ~six dye molecules per antibody molecule.

For ratiometric imaging, cells were dual labeled with a 1:1 mixture of the Licor-HER2 mAb (785-nm excitation) and the AF647-isotype control mAb

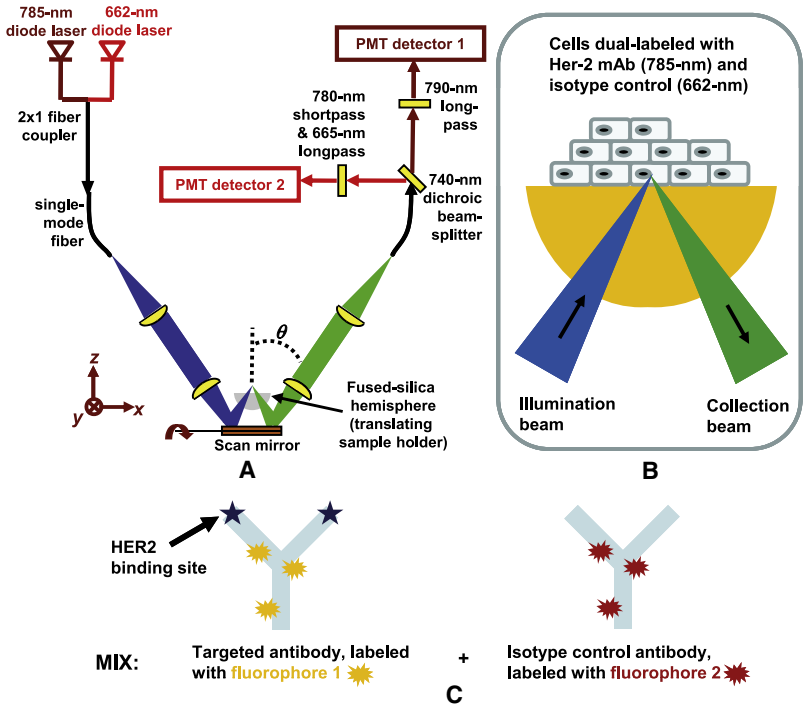

FIGURE 1 Imaging setup. (*A*) The two-color DACM with fluorescence excitation at 662 nm and 785 nm. (*B*) Cultured cells and tissue samples are placed on the hemispherical DACM sample holder and imaged in three dimensions. (*C*) HER2-targeted antibodies and isotype-control antibodies are labeled with different fluorophores and mixed 1:1 for the dual labeling of cells and tissue samples.

(662-nm excitation). 1×10^6 cells were reacted with 2 μg of each of the labeled antibodies in a 20 μL volume for 1 h. The cells were rinsed in 1 mL of PBS, spun down at 300 $\times$ *g* for 5 min, and then resuspended in 100 μL PBS.

For flow cytometric analyses, 10^6 cells were reacted with 2 μg of either the Licor-HER2 mAb or the AF647-isotype control mAb (662-nm excitation). To compare antibody binding affinities accurately using a single emission/detection channel in the flow cytometer, a secondary anti-isotype fluorescent antibody (2 μg; ab6785, Abcam, Cambridge, MA) was used to identically label both of the primary antibodies (anti-HER2 and isotype control). The secondary antibody, excited at 488 nm, was a FITC-labeled Goat polyclonal to Mouse IgG antibody. Flow cytometry was performed on a Becton Dickinson FACSCalibur (Franklin Lakes, NJ) and data analyzed with FlowJo software (Ashland, OR).

Matrigel suspensions

For 3D imaging, HER2-positive cells were suspended in BD Matrigel Basement Membrane Matrix. SKBR3 cells (1×10^3) were dual labeled with 2 μg of each of the labeled antibodies in a 20-μL volume for 1 h. The cells were then rinsed in 1 mL of PBS, spun down at 300 $\times$ *g* for 5 min, and resuspended in 100 μL of Matrigel at 4°C. The Matrigel matrix was then allowed to warm up to 25°C, where it quickly gelatinized.

To simulate a nonspecific background, a 1:1 mixture of the labeled antibodies was introduced into the Matrigel matrix before introducing the labeled cells. Specifically, 1 μg of both the Licor-HER2 mAb and the AF647-isotype control mAb were added into 100 μL of Matrigel matrix. 1×10^6 labeled cells were then suspended into this matrix.

Frozen human breast cancer specimens

Snap-frozen, breast cancer tumor specimens, along with corresponding normal breast tissue specimens from the same patient, were obtained from the Stanford Tissue Bank. These tissues were embedded in optimal cutting temperature (OCT) compound. HER2/neu expression levels were confirmed by standard fluorescence in situ hybridization methods by the pthology department at Stanford. Breast tumors with clinically elevated HER2 levels, as indicated by fluorescence in situ hybridization analysis, as well as HER2-negative breast tumors, were imaged with 3D ratiometric microscopy. For 3D microscopy, a small (2 $\times$ 2 $\times$ 2 mm) cube of tissue was cut out of the frozen specimen, taking care to remove the tissue from the OCT frozen tissue matrix. As the tissue thawed out on a glass slide, a drop (2–3 μL) of the 1:1 mixture of labeled antibodies (500 nM concentration of each fluorescent antibody) was applied to the tissue and allowed to soak into the tissue for 1 min. Dimethyl sulfoxide was added to the antibody solution to 5% final concentration to facilitate penetration into the thick tissue specimen. After the tissue was soaked in the antibody solution, it was irrigated with PBS for 30 s to remove unbound probe. The tissue was then placed on the sample holder of the dual-axis confocal microscope (DACM) and imaged.

Two-color DACM

A detailed description of the theory and imaging performance of a DACM for deep-tissue optical sectioning has been published previously (20,21). As illustrated in Fig. 1 *A*, the two-color tabletop system incorporates two diode lasers, at 662 nm and 785 nm, which are coupled into one single mode fiber (Corning HI780, Corning, NY). To increase the signal collection efficiency, a slightly multimode fiber (SMF28), with a core diameter of 8.3 μm, is used as the collection fiber for our DACM at the expense of a slight degradation in the normally diffraction-limited performance, resulting in a spatial resolution of 5-μm transverse and 7-μm axial (full width at half-maximum). The collected light is collimated in free space and sent through a dichroic beam splitter (Semrock, Rochester, NY, FF740-Di01-25 $\times$ 36) and the appropriate filters (Semrock SP01-785RU-25 and LP02-664RU-25 for the AF647 channel; Semrock LP02-785RU-25 for the IRDye 800CW channel) to separate the two fluorescent signals originating from each fluorophore into two separate multimode fibers (50-μm core). Two fiber-coupled Hamamatsu (Hamamatsu, Japan) photomultiplier tubes (H7422-50) are used for simultaneous detection of the two imaging channels, with each detector sending data to a separate 8-bit frame grabber (Data Translation DT3152, Marlborough, MA). The acquisition triggers, along with the horizontal- and vertical-sync signals, are identical for both frame grabbers to insure image coregistration. In addition, the achromatic DACM optics lead to a negligible offset in the focal volumes for each wavelength.

In this study, the DACM provided vertical image sections, at a 2-Hz frame rate, that were 600 μm wide by 320 μm deep (1000 $\times$ 420 pixels). For 3D

imaging, 300 vertical sections were acquired serially at 1-μm increments for a total horizontal field of view of 600 $\times$ 300 μm (1000 $\times$ 300 pixels).

Quantitative ratiometric microscopy and calibration

For quantitative ratiometric imaging of fluorescently labeled cells, cell suspensions were applied to a microscope sample holder and allowed to settle and form several cell layers, as illustrated in Fig. 1 *B*. For 3D imaging of cells suspended in matrigel, the gelatinized cell suspensions were placed on top of the microscope sample holder and imaged. Fig. 1 *C* depicts the two-color dual-label contrast agent mixture used for this technique.

Before, or immediately after, the imaging of cell cultures or tissue specimens, the two-color DACM was calibrated by imaging a diluted sample of the 1:1 fluorescent antibody solution. The exact same laser intensity set points and detector gain settings were used to image the 1:1 antibody mixture as were used to image the labeled cell culture or tissue specimens. The ratio of the average image intensity from each channel was measured and used as a calibration factor to quantify the biological images. Additional details on calibration and image processing, along with a discussion of the mathematical model and assumptions used for this technique, may be found in Appendix A.

Image processing

The theory behind our ratiometric technique is covered in greater detail in Appendix A. For image processing, 3D image stacks (300 vertical sections) were imported into an image-rendering software package (Amira 4.1, Carlsbad, CA). Horizontal, en-face view projections (averaged in the vertical *z*-direction), 5 pixels deep, were constructed in Amira to improve the signal/noise ratio (SNR) of the images. Based on the sampling conditions of our DACM, 5 pixels correspond to 3.8 μm in the vertical direction, which is slightly greater than half the full width at half-maximum axial resolution of the DACM (7 μm). Therefore, the Nyquist sampling criteria is nearly satisfied with a 5-pixel projection, insuring minimal loss of information.

Horizontal projections from both image channels were imported into MATLAB (The MathWorks, Natick, MA), where a threshold routine was first applied to each image to ignore saturated pixels (intensity of 256) as well as pixels within the noise floor (intensity of <5). A pixel-by-pixel ratio image was then constructed from the two image channels (antibody-targeted and isotype control image). Finally, a predetermined calibration factor was applied to the ratiometric image. Ratiometric images were then quantitatively displayed using a false color look up table and rendered volumetrically in Amira 4.1.

RESULTS

Two-color DACM

For quantitative ratiometric imaging of fluorescently labeled cells, cell suspensions were applied to the DACM sample holder and allowed to settle and form several cell layers, as illustrated in Fig. 1 *B*. Cells suspended in matrigel, as well as human tissues, were also placed on top of the microscope sample holder and volumetrically imaged. Fig. 1 *C* depicts the two-color dual-label contrast agent mixture used for this technique.

Quantitative imaging of cell culture and comparison with flow cytometry

For preliminary studies using HER2-positive breast cancer cell lines, efficient antibody labeling and rinsing away of unbound probe was expected. Therefore, the gain setting for the HER2 channel of the DACM was intentionally lowered, with respect to the isotype-control channel, in anticipation of the large signal level from the HER2-antibody channel. A calibration factor of 0.118 was measured, according to the protocol described in the Methods section, reflecting the low gain setting of the HER2 channel. Due to the limited, 8-bit- (256 level-) dynamic range of our frame grabbers, it was necessary to carefully adjust the gain setting in all our experiments to insure adequate SNR in our ratiometric images. Future systems, optimized for this technique, will utilize higher dynamic range frame grabbers (12–16 bits) for improved SNR and will be less dependent upon initial gain settings (see Appendix B).

Fig. 2 *A* is a quantitative image, of the ratio between the amount of HER2 antibody versus isotype control, of a horizontal projection (5 pixels deep, see Methods) of SKBR3 cells deposited on the DACM sample holder. Note that the ratiometric image displays $C_{\text{specific}}/C_{\text{nonspecific}} - 1$, rather than simply the concentration ratio between the targeted probe (specific) versus the nonspecific control probe: $C_{\text{specific}}/C_{\text{nonspecific}}$. In the absence of specific binding, $C_{\text{specific}} = C_{\text{nonspecific}}$ and $C_{\text{specific}}/C_{\text{nonspecific}} = 1$. Therefore displaying $(C_{\text{specific}}/C_{\text{nonspecific}} - 1)$ in ratiometric images allows for more effective image interpretation in which zero specific binding is indicated as zero image intensity.

The image histogram in Fig. 2 *B* indicates that the distribution in the ratio, between HER2 antibody versus isotype control, peaks at ~50. Flow cytometric data obtained for the exact same cells used for ratiometric imaging, are shown in Fig. 2 *C*. The difference in the fluorescence intensity peaks, between the anti-HER2-mAb-labeled cells, and the isotype-control-labeled cells, is ~50-fold and in excellent agreement with the quantitative imaging results. For flow cytometry, as described in the Methods section, a FITC-labeled goat anti-mouse IgG secondary antibody was used to label both the HER2 and isotype-control primary antibodies attached to the SKBR3 cell surfaces. Therefore, since a single emission/detection channel was used for all flow analyses, the fluorescence intensities shown in Fig. 2 *C* directly correlate with the two antibody concentrations.

In addition to the SKBR3 cell line, which exhibits strong and uniform HER2 expression, we also utilized the MDA-HER2 cell line that exhibits a weaker and more variable cell-surface expression level for HER2. Fig. 3 displays imaging and flow cytometry results, for the MDA-HER2 cell line, that are analogous to those in Fig. 2 for the SKBR3 cell line. Both the ratiometric image, as well as the flow-cytometry histogram, indicates a nonuniform distribution in HER2 expression. However, the ratio between the peak levels of HER2 antibody versus isotype control is ~20 for both sets of data. Note that the image histogram in Fig. 4 *B* becomes noisier at the lowest ratios because of the limited 8-bit dynamic range of the frame grabbers used in these experiments, coupled with the gain settings chosen for acquiring this set of data.

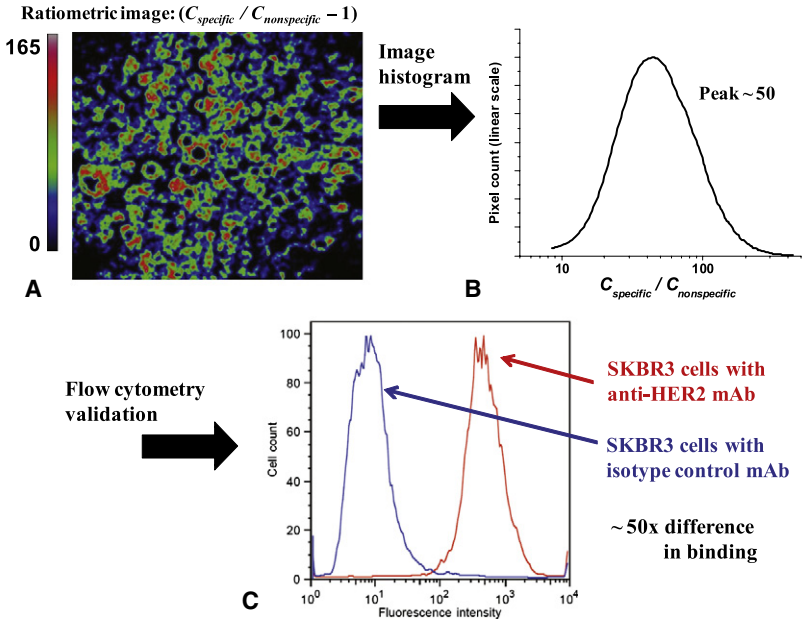

FIGURE 2 Quantitative imaging of SKBR3 cells. (*A*) A ratiometric image of a ~10-μm thick horizontal (en-face view) projection of SKBR3 cells. Pixel intensities correspond to the ratio in the concentration of targeted HER2 antibody versus isotype control antibody. (*B*) A histogram of the pixel intensities in the ratiometric image reveals a peak ratio of ~50. (*C*) Flow cytometry validations (see Methods) indicate a ~50× greater binding affinity of the anti-HER2 mAb versus the isotype control.

As a control study of the specificity of our HER2 antibody, HER2-negative cells (MDA-NEO) were also labeled with our dual-antibody mixture. Ratiometric imaging and flow cytometry studies both revealed negligible differences between the anti-HER2 mAb and the isotype control (not shown).

3D cell suspensions in matrigel

To demonstrate the ability to perform our quantitative imaging technique in three dimensions, as well as to investigate the potential for reducing nonspecific background signals, we suspended antibody-labeled SKBR3 cells in matrigel. A 1:1 mixture of our targeted antibody (channel 1) and isotype control antibody (channel 2) was mixed into the matrigel (see Methods) to simulate a nonspecific background. A volume rendering of the image from channel 1 alone (targeted antibody) is shown in Fig. 4 *A*. The strongly stained SKBR3 cells are visible, but are obscured by the presence of a nonspecific background within the Matrigel. Fig. 4 *B* displays an analogous volume rendering, after ratiometric image processing. In addition to providing a quantitative 3D map of the ratio between the amount of HER2 antibody versus isotype control, a significant reduction in the nonspecific background is evident, leading to improved image interpretation.

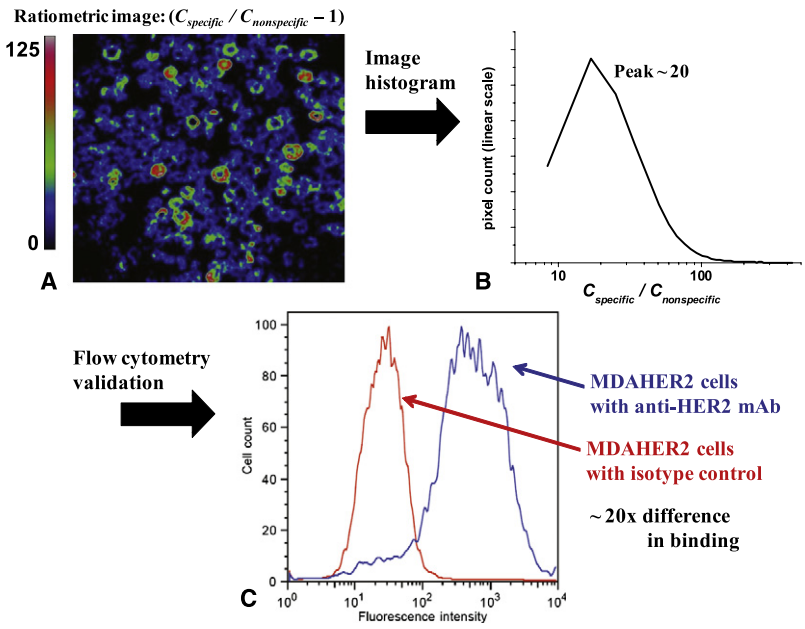

FIGURE 3 Quantitative imaging of MDA-HER2 cells. (*A*) A ratiometric image of a ~10-μm thick horizontal (en-face view) projection of MDA-HER2 cells. Pixel intensities correspond to the ratio in the concentration of targeted HER2 antibody versus isotype control antibody. (*B*) A histogram of the pixel intensities in the ratiometric image reveals a peak ratio of ~20. (*C*) Flow cytometry validations (see Methods) indicate a nonuniform expression of HER2 that results in a peak concentration of anti-HER2 mAb that is ~20× the concentration of the isotype control.

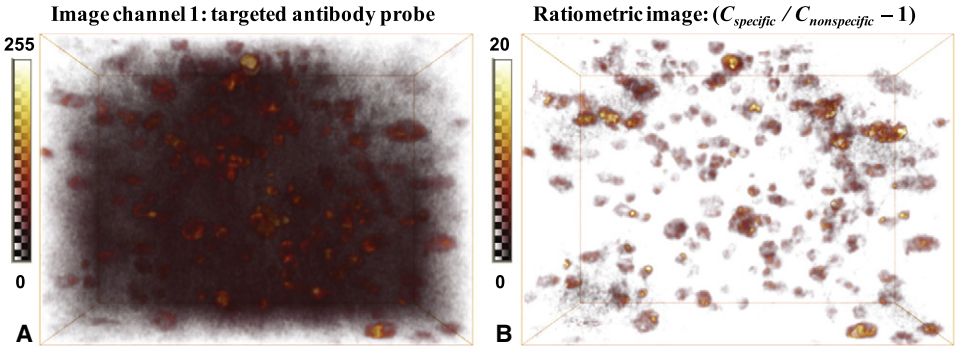

FIGURE 4 3D quantitative microscopy of suspended cells. (*A*) A volume rendering of channel 1 (HER2-targeted mAb only), revealing a significant amount of nonspecific background signal (see Methods) obscuring the cells. (*B*) A volume rendering after ratiometric image processing, demonstrating a significant reduction in nonspecific background as well as a quantitative map of the ratio between anti-HER2 mAb versus isotype control.

3D imaging of human breast tissue specimens

As a final demonstration of our ratiometric technique, we obtained snap-frozen specimens of HER2-positive and HER2-negative breast cancers, along with normal breast tissue samples from the corresponding patients. The tissues were stained with our dual-antibody mixture (see Methods) and rinsed in PBS before imaging. Fig. 5, *A* and *B*, show results from a normal breast tissue sample, Fig. 5, *C* and *D*, are images from a HER2-negative breast tumor, and Fig. 5, *E* and *F*, are images from a HER2-positive breast tumor. Fig. 5 *A* is a volume rendering of image channel 1 (targeted antibody alone), indicating that a significant amount of antibody has accumulated within the normal breast tissue sample. However, once ratiometric image processing is performed (Fig. 5 *B*), it is evident that the antibody accumulation is largely nonspecific. Fig. 5 *C* is a volume rendering of image channel 1 for a breast tumor specimen. Ratiometric image processing, shown in Fig. 5 *D*, helps to remove much of the nonspecific background and reveals a low expression level for HER2/neu. Fig. 5 *E* is a volume rendering, of image channel 1, for a breast tumor specimen. Ratiometric image processing, shown in Fig. 5 *F*, helps to remove much of the nonspecific background and quantitatively confirms an elevated HER2/neu expression level.

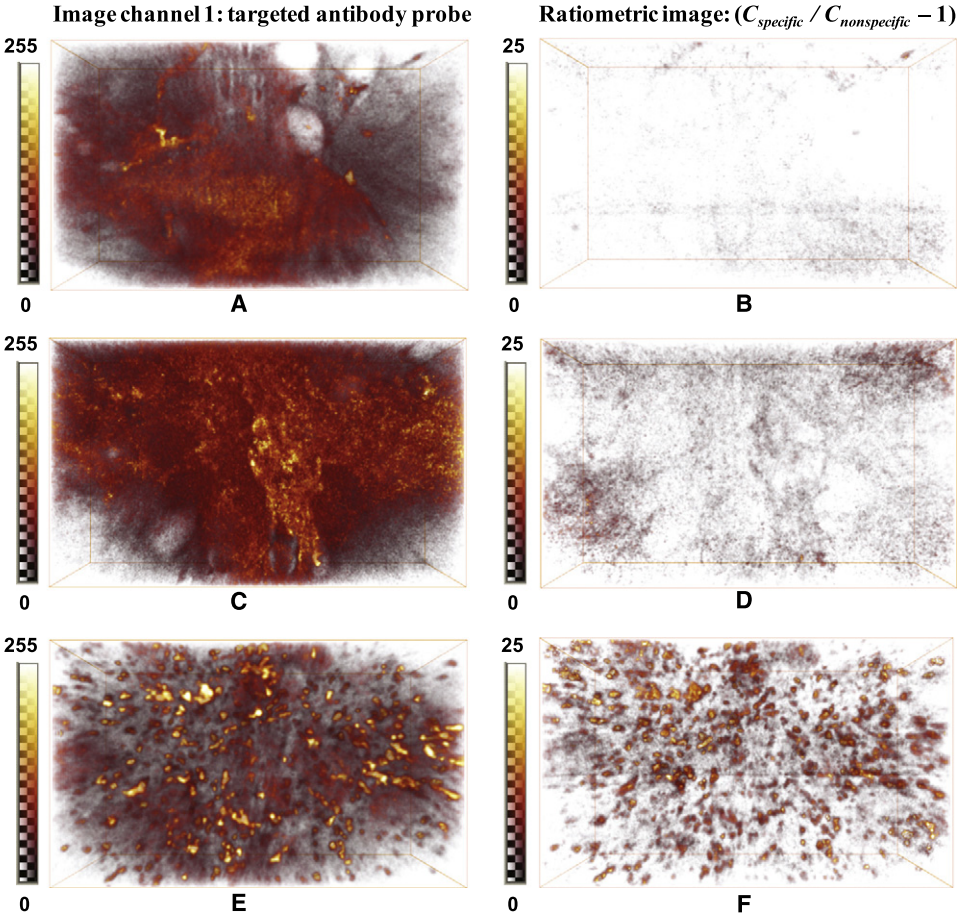

FIGURE 5 3D quantitative microscopy of human breast cancer and normal samples. (*A*) Normal breast tissue: a volume rendering of channel 1 (targeted antibody probe), revealing significant probe accumulation. (*B*) Normal breast tissue (same volume as *A*): a volume rendering, after ratiometric image processing, which reveals minimal signal that is molecularly specific to the HER2/neu receptor. (*C*) HER2-negative breast cancer: a volume rendering of channel 1 (targeted antibody probe), revealing significant probe accumulation. (*D*) HER2-negative breast cancer (same volume as *C*): a volume rendering, after ratiometric image processing, demonstrating removal of nonspecific background. The ratiometric image indicates low levels of HER2/neu expression. (*E*) HER2-positive breast cancer: a volume rendering of channel 1 (targeted antibody probe). (*F*) HER2-positive breast cancer (same volume as *E*): a volume rendering, after ratiometric image processing, demonstrating a significant reduction in nonspecific background as well as a quantitative map of the ratio between anti-HER2 mAb probe versus isotype control probe. Elevated HER2/neu expression is confirmed and quantified.

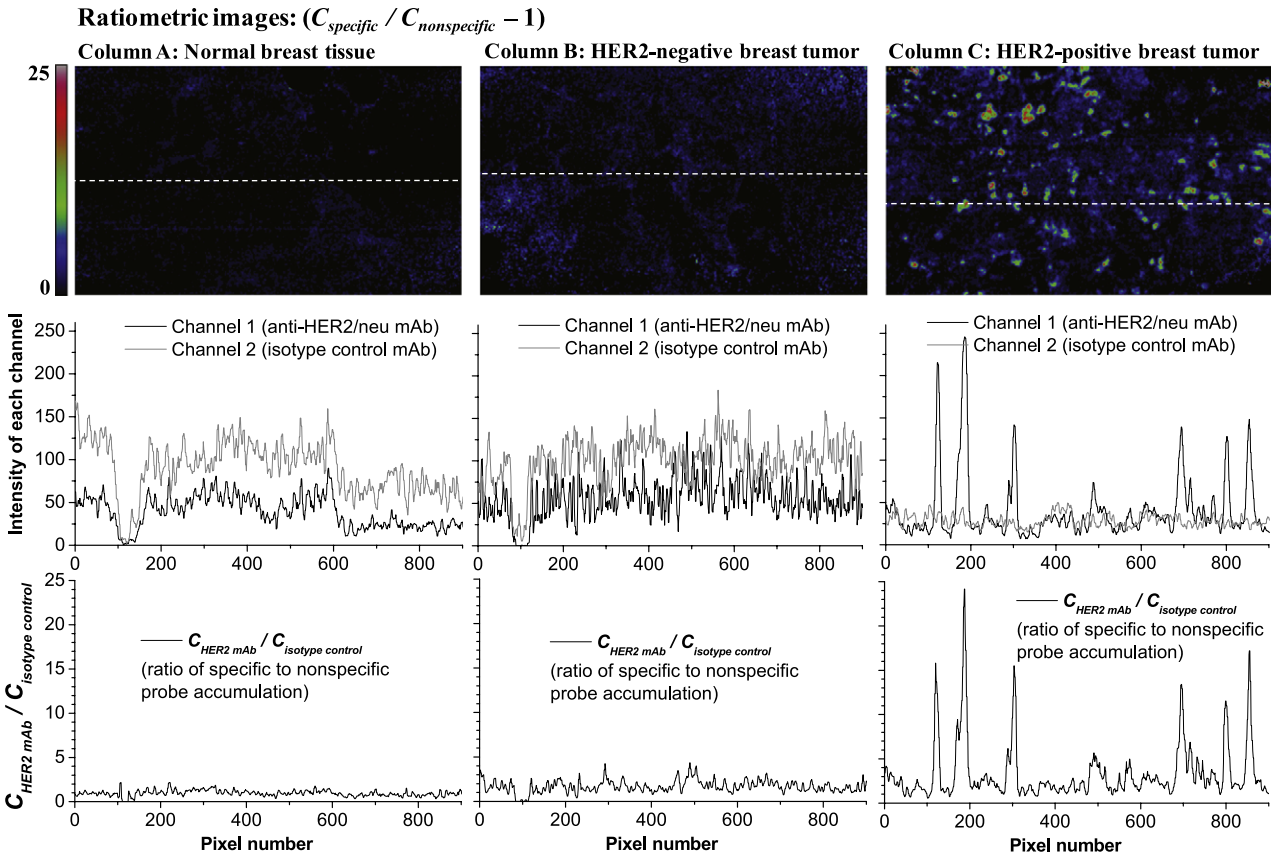

FIGURE 6 Ratiometric optical sections, with line profiles. Line profile data are shown for the row of pixels indicated on the ratiometric optical sections. The optical sections shown are 25 μm beneath the tissue surface and are taken from the same volumetric data set shown in Fig. 5. Line profiles are shown for both raw imaging channels (channel 1, targeted antibody and channel 2, isotype control) as well as the calibrated ratiometric image. Note that the images display ($C_{\text{specific}}/C_{\text{nonspecific}} - 1$) whereas the ratiometric line profiles display $C_{\text{specific}}/C_{\text{nonspecific}}$. Column *A* (*left*) shows data from normal breast tissue. Column *B* (*center*) shows data from a HER2-negative breast tumor. Column *C* (*right*) shows data from a HER2-positive breast tumor. See text for details.

In Fig. 6, individual ratiometric image sections, from the volumetric data shown in Fig. 5, are shown for normal breast tissue, HER2-negative breast cancer, and HER2-positive breast cancer. These horizontal (en-face) optical sections are all located 25 μm beneath the tissue surface. Line profile data are shown for the row of pixels indicated by a horizontal line in the images. The first row of plots beneath the images displays line profile data from both raw image channels. Channel 1 is the fluorescence signal from the HER2-specific probe whereas channel 2 is the signal from the nonspecific isotype control probe. The plots at the bottom row represent line profiles of the calibrated ratiometric data. Note that the ratiometric images display $C_{\text{specific}}/C_{\text{nonspecific}} - 1$, whereas the ratiometric line profiles display $C_{\text{specific}}/C_{\text{nonspecific}}$. As mentioned previously, in the absence of specific binding, $C_{\text{specific}} = C_{\text{nonspecific}}$ and $C_{\text{specific}}/C_{\text{nonspecific}} = 1$. Therefore displaying $C_{\text{specific}}/C_{\text{nonspecific}} - 1$ in the ratiometric images allows for more effective image interpretation in which zero specific binding is indicated as zero image intensity.

From the line profiles shown in Fig. 6, the two major advantages of our ratiometric imaging scheme are apparent. First, it is possible to reduce the ambiguity in image interpretation due to nonspecific sources of contrast. For example, in column *A* of Fig. 6, the channel 1 line profile for the normal breast tissue optical section shows a large dip in intensity at around pixel number 110, and also shows a drop in intensity above pixel number 600. Since channel 2 exhibits an analogous profile, the resulting ratiometric line profile reveals that these intensity changes are not due to specific binding of the anti-HER2 imaging probe. In addition to removing ambiguous nonspecific sources of differential contrast, the second benefit of our technique is that it is quantitative. For example, in column *B* of Fig. 6, channel 1 shows a fairly uniform staining intensity across the line profile (with the exception of a dip at around pixel 100). In the absence of a calibrated control, this signal could be interpreted either as a uniformly high level of specific probe accumulation, or as a uniform nonspecific accumulation of the imaging probe. By performing calibrated ratiometric microscopy, the intensity of the probe may be quantified with respect to a nonspecific control. In the case of the HER2-negative breast tumor imaged in column *B*, the quantitative results indicate a very low level of HER2-specific probe accumulation. Similarly, the ratiometric line profile in column *C* of Fig. 6 clearly

reveals and quantifies the level of specific probe accumulation relative to a nonspecific control.

Nonuniformity and uncertainty

One nonideal feature of the DACM used in this study is that signal intensities drop off slightly at the edges of the field of view, owing to scanning-induced optical aberrations. Ratiometry helps to counteract nonuniformities such as this because even though the raw signals intensities are falling off in both channels, their ratio is insensitive to such common-mode losses and remains accurate. SNR does degrade as the raw signal levels drop. This is accounted for in the image-processing algorithm by removing all pixels that are below a certain signal threshold (<5 out of 256 grayscales). Therefore, at the edges of the ratiometric images, more pixels are given a value of zero (*black* on the color map). Nevertheless, the ratiometric image histograms maintain an accurate shape because they neglect zero-valued pixels, although the distributions become noisier as the raw signal levels drop.

An analysis of the effects of noise sources, such as digitization noise (bit noise), on this quantitative method is performed in Appendix B. For a frame grabber with an 8-bit dynamic range, as used in this study, digitization noise alone accounts for at least a 1% uncertainty in the ratiometric result. This is for a best-case scenario in which the system gain settings are optimally set such that the raw signal levels fall at the center of the dynamic range of the frame grabbers. In practice, when imaging a heterogeneous sample with any contrasting features, the uncertainty due to digitization noise is much worse (see Appendix B). For a 12-bit frame grabber, which is preferred for future studies, the digitization-induced uncertainty is more than an order of magnitude lower. As mentioned previously, our image processing algorithm removes all pixels with a signal intensity of <5 out of 256 pixels. At such low signal levels, the uncertainty due to digitization noise is at least 20% and is unacceptable for reliable ratiometry. Additional noise sources, such as laser, detector, and shot noise (which propagate according to Eq. B.3 in Appendix B) should be carefully considered when utilizing this technique to insure robust quantification of probe concentrations.

DISCUSSION

We have developed a ratiometric image-processing method to quantify cellular biomarker expression and to reduce the confounding effects of nonspecific probe accumulation for microscopic analyses of thick or intact tissues. This technique is designed to address recent challenges in in vivo 3D microscopy, in which topical application and rinse-removal of imaging probes is nonuniform and inefficient, leading to misleading signals that are not molecularly specific. To demonstrate this two-color ratiometric technique, a monoclonal antibody is used to target the HER2/neu tyrosine kinase receptor that is often overexpressed in breast tumors. However, this technique is not limited to antibody-based imaging probes and should have utility for other targeting moieties such as peptides. With peptide imaging probes, a suitable negative-control peptide, such as a scrambled peptide, would need to be used with similar nonspecific binding characteristics as compared to the targeting peptide. These smaller molecular probes would diffuse into and out of tissues more readily and offer advantages for tissue staining and in vivo imaging.

In this study, we have presented data using HER2-positive cell cultures that demonstrate the accuracy of our calibrated image-processing technique to quantify the ratio between molecularly targeted versus nonspecific probe accumulation. Our imaging results, of labeled breast cancer cells, compare favorably with quantitative flow cytometry analysis. We have also suspended labeled cells in Matrigel, and have simulated a nonspecific background within the Matrigel, to demonstrate the ability of our technique to quantify biomarker expression levels in three dimensions and to greatly reduce the effects of a nonspecific background. Finally, we have demonstrated this technique on thick samples of excised human breast cancer and normal breast tissue. By performing calibrated ratiometric image processing, we demonstrate the ability to quantify specific probe binding and to reduce ambiguity due to nonspecific probe accumulation. This quantitative imaging technique improves the ability to distinguish normal tissue and HER2-negative tumors from HER2-positive tumors in thick tissue 3D microscopy, in which the staining and rinsing away of contrast agents is inefficient. As such, these data indicate that microscopic analyses of entire tissue biopsies could be performed rapidly and in close proximity to the patient, and reveal both the presence and extent of biomarker expression throughout the entire sample. This would be useful for diagnosis and guiding therapy, could be easily automated, and would remove sampling errors that occur in analyzing selected sections of a tissue.

A number of major assumptions, detailed in Appendix A, must be satisfied to maintain the accuracy of our ratiometric technique. Although we have presented data demonstrating the feasibility of this technique, certain improvements could be made to optimize future results. As mentioned in the Results section, frame grabbers with a higher dynamic range (at least 12 bits) are needed to improve the SNR of the ratiometric images, and to reduce the sensitivity of this technique to initial laser and detector gain settings. In these studies, two near-infrared cyanine dyes were used: Alexa Fluor 647 and LI-COR IRDye 800CW. Although these dyes are structurally similar, it is important to carefully study and optimize our choice of fluorescent dyes in the future to insure similar behavior in tissues. The structure, polarity, and steric configuration of the dyes should be as similar as possible to minimize dye-associated differences between the targeted and

negative-control imaging probes. This similarity in the dyes is particularly important if small-molecule targeting agents such as peptides are to be used, since the dye molecules (~1 kDa) will play a much larger role in the binding dynamics and diffusion of such small-molecule probes (~1–10 kDa), as compared to large antibodies (150 kDa). Finally, whether small-molecule or antibody probes are utilized, the ability to distinguish between specific and nonspecific binding depends upon the accuracy of the negative-control to mimic the nonspecific effects of the targeted probe. As with flow cytometry, care must be taken to develop appropriate positive and negative probes for this purpose, especially as novel small-molecule reagents are utilized.

The technique described in this article was developed specifically to address challenges in image interpretation during in vivo and ex vivo 3D microscopy of thick intact tissues with topically applied molecular contrast agents. By attenuating the effects of nonspecific background signals caused by ineffective probe application and rinsing, and by providing quantification of specific probe binding relative to nonspecific binding, this ratiometric method is an important step toward the larger goal of in vivo optical biopsy and accurate real-time histopathology of intact tissue samples. The ability to quantitatively visualize molecular biomarkers in unfixed and intact tissues, through the use of advanced microscopy techniques coupled with digital image processing, represents what we believe is an exciting new approach to disease detection and pathology with the potential to accelerate the analysis, increase the accuracy, and reduce the cost associated with disease diagnosis.

APPENDIX A: MODEL AND ASSUMPTIONS

Voxel intensities, S_i, for each wavelength channel, i, may be expressed as

$$S_i = G_i \cdot n_i \cdot c_i \cdot I_i \cdot \sigma_i \cdot \chi_i, \tag{A1}$$

where:

G_i = electronic gain and system constants (optical efficiency, detector quantum yield, etc.).
n_i = average number of dye molecules per antibody.
c_i = concentration of antibody (or generic targeted contrast agent).
I_i = laser intensity at voxel volume.
σ_i = absorption cross-section of dye.
χ_i = fluorescence yield of dye.

A number of assumptions must be true to maintain the accuracy of the calibrated ratiometric image-processing technique used in this study:

1. The ratio of the laser intensities is constant (i.e., $\frac{I_1}{I_2}$ is constant) throughout the imaged volume. With achromatic optics, both wavelengths travel identical paths within the tissue. If we assume that absorption is negligible compared to scattering losses (true for the near-infrared (NIR) wavelengths used), then the ratio in the laser intensities will be constant with imaging depth if the scattering coefficient is the same for both wavelengths. Although the scattering coefficient does vary as a function of wavelength, we are assuming that this difference is negligible over the few hundred microns of depth that we are imaging. Note: if both fluorophores were excited with one laser source, as could be possible if quantum dots were used, then $\frac{I_1}{I_2} = 1$.
2. There is negligible crosstalk between channels, due to poor filtering, FRET effects, etc.
3. There is negligible autofluorescence (we use NIR wavelengths to avoid autofluorescence).
4. There is negligible variation in absorption cross section and fluorescence yield of the dye in the sample.
5. The dye labeling is dense enough that ensemble averages are valid for each voxel (i.e., the average number of dye molecules per antibody, n_i, does not vary for each voxel).

Assume that we have a two-color multispectral system, with fluorophores 1 and 2. If the optical alignment and gain settings of the DACM are fixed, and if assumptions 1–5 above are satisfied, then we can say that for each voxel, $\frac{k_1}{k_2}$ is a constant, where $k_i = G_i \cdot n_i \cdot I_i \cdot \sigma_i \cdot \chi_i$.Therefore,

$$\frac{S_1}{S_2} = \frac{G_1 \cdot n_1 \cdot c_1 \cdot I_1 \cdot \sigma_1 \cdot \chi_1}{G_2 \cdot n_2 \cdot c_2 \cdot I_2 \cdot \sigma_2 \cdot \chi_2} = \left(\frac{k_1}{k_2}\right)\left(\frac{c_1}{c_2}\right). \tag{A2}$$

The calibration constant, $\frac{k_1}{k_2}$, is measured by imaging a 1:1 mixture of dye-labeled antibody, where $\frac{c_1}{c_2} = 1$. Once the calibration factor is measured, ratiometric image processing (see Methods) is used to quantify the ratio of antibody-targeted contrast agent versus isotype control for each voxel:

$$R = \frac{c_1}{c_2} = \frac{c_{\text{antibody}}}{c_{\text{isotype}}} = \left(\frac{k_2}{k_1}\right)\frac{S_1}{S_2}. \tag{A3}$$

APPENDIX B: UNCERTAINTY ANALYSIS

For each voxel in channel i, there is an average value $\overline{S}_i$ with an associated uncertainty δS_i such that

$$S_i = \overline{S}_i \pm \delta S_i. \tag{B1}$$

The ratio, R, defined in (A.3), may also be expressed as

$$R = R \pm \delta R. \tag{B2}$$

The fractional uncertainties, if due to independent noise sources, propagate according to

$$\frac{\delta R}{\overline{R}} = \sqrt{\left(\frac{\delta S_1}{S_1}\right)^2 + \left(\frac{\delta S_2}{S_2}\right)^2}. \tag{B3}$$

To analyze the effects of digitization noise, we define n = bit depth where the number of digitization levels (i.e., grayscales) is 2^n. With optimized gain settings, the average signal level is at approximately half the full dynamic range: $1/2(2^n) = 2^{n-1}$. The fractional uncertainty due to digitization noise in this case is $1/(2^{n-1})$. Therefore, the best-case uncertainty in the ratiometric output is

$$\frac{\delta R}{\overline{R}} = \sqrt{\left(\frac{1}{2^{n-1}}\right)^2 + \left(\frac{1}{2^{n-1}}\right)^2} = \frac{\sqrt{2}}{2^{n-1}}. \tag{B4}$$

Thus, for an 8-bit frame grabber, $\frac{\delta R}{\overline{R}} \geq 1.1\%$, whereas for a 12-bit digitizer, $\frac{\delta R}{\overline{R}} \geq 0.07\%$.

Assume that we are imaging a tumor margin, or a specific tissue component, using a molecular imaging probe that offers a contrast ratio of r. In the best case scenario, with optimized gain settings, the negative-control channel (channel 2) as well as the positive signal levels in channel 1 are detected by an n-bit frame grabber at a level of approximately 2^{n-1}. The negative signal levels in channel 1 are recorded at approximately $2^{n-1}/r$. The fractional uncertainties due to digitization are $1/2^{n-1}$ and $r/2^{n-1}$,

respectively. The uncertainty in the resulting ratiometric image is limited by the low negative signal level in channel 1:

$$\frac{\delta R}{\overline{R}} = \sqrt{\left(\frac{1}{2^{n-1}}\right)^2 + \left(\frac{r}{2^{n-1}}\right)^2} = \frac{\sqrt{1 + r^2}}{2^{n-1}}. \qquad \text{(B5)}$$

If the contrast ratio is $r = 5$, then for an 8-bit digitizer, $\frac{\delta R}{\overline{R}} \geq 4\%$, whereas for a 12-bit digitizer, $\frac{\delta R}{\overline{R}} \geq 0.25\%$.

Other noise sources, such as shot noise, detector noise, and electronic noise, also propagate according to Eq. B3 and will contribute to the reliability of R. Ideally, fluorescence signals should be detected with SNR comparable to or better than the SNR due to digitization noise, as described above.

This work was funded in part by a grant from the National Institute of Health, U54 CA105296 (National Cancer Institute) Network for Translational Research in Optical Imaging. J.T.C.L. was supported in part by a Canary Foundation/American Cancer Society postdoctoral fellowship for early cancer detection.

REFERENCES

1. Flusberg, B. A., E. D. Cocker, W. Piyawattanametha, J. C. Jung, E. L. M. Cheung, et al. 2005. Fiber-optic fluorescence imaging. *Nat. Methods.* 2:941–950.
2. Fujimoto, J. G., M. E. Brezinski, G. J. Tearney, S. A. Boppart, B. Bouma, et al. 1995. Optical biopsy and imaging using optical coherence tomography. *Nat. Med.* 1:970–972.
3. Tearney, G. J., M. E. Brezinski, B. E. Bouma, S. A. Boppart, C. Pitris, et al. 1997. In vivo endoscopic optical biopsy with optical coherence tomography. *Science.* 276:2037–2039.
4. Myaing, M. T., D. J. MacDonald, and X. Li. 2006. Fiber-optic scanning two-photon fluorescence endoscope. *Opt. Lett.* 31:1076–1078.
5. Carlson, K., M. Chidley, K.-B. Sung, M. Descour, A. Gillenwater, et al. 2005. In vivo fiber-optic confocal reflectance microscope with an injection-molded plastic miniature objective lens. *Appl. Opt.* 44:1792–1797.
6. Kiesslich, R., J. Burg, M. Vieth, J. Gnaendiger, M. Enders, et al. 2004. Confocal laser endoscopy for diagnosing intraepithelial neoplasias and colorectal cancer in vivo. *Gastroenterology.* 127:706–713.
7. Liu, J. T. C., M. J. Mandella, H. Ra, L. K. Wong, O. Solgaard, et al. 2007. Miniature near-infrared dual-axes confocal microscope utilizing a two-dimensional microelectromechanical systems scanner. *Opt. Lett.* 32:256–258.
8. Hsiung, P.-L., J. Hardy, S. Friedland, R. Soetikno, C. B. Du, et al. 2008. Detection of colonic dysplasia *in vivo* using a targeted heptapeptide and confocal microendoscopy. *Nat. Med.* 14:454–458.
9. Wang, T. D., S. Friedland, P. Sahbaie, R. Soetikno, P. L. Hsiung, et al. 2007. Functional imaging of colonic mucosa with a fibered confocal microscope for real-time in vivo pathology. *Clin. Gastroenterol. Hepatol.* 5:1300–1305.
10. Grynkiewicz, G., M. Poenie, and R. Y. Tsien. 1985. A new generation of Ca^{2+} indicators with greatly improved fluorescence properties. *J. Biol. Chem.* 260:3440–3450.
11. Stricker, S. A., and M. Whitaker. 1999. Confocal laser scanning microscopy of calcium dynamics in living cells. *Microsc. Res. Tech.* 46:356–369.
12. Bright, G. R., G. W. Fisher, J. Rogowska, and D. L. Taylor. 1987. Fluorescence ratio imaging microscopy: temporal and spatial measurements of cytoplasmic pH. *J. Cell Biol.* 104:1019–1033.
13. Jares-Erijman, E. A., and T. M. Jovin. 2003. FRET imaging. *Nat. Biotechnol.* 21:1387–1395.
14. Burgstahler, R., H. Koegel, F. Rucker, D. Tracey, P. Grafe, et al. 2002. Confocal ratiometric voltage imaging of cultured human keratinocytes reveals layer-specific responses to ATP. *Am. J. Physiol. Cell Physiol.* 284:944–952.
15. Sinaasappel, M., and H. J. C. M. Sterenborg. 1993. Quantification of the hematoporphyrin derivative by fluorescence measurement using dual-wavelength excitation and dual-wavelength detection. *Appl. Opt.* 32:541–548.
16. Bogaards, A., M. C. G. Aalders, A. J. L. Jongen, E. Dekker, and H. J. C. M. Sterenborg. 2001. Double ratio fluorescence imaging for the detection of early superficial cancers. *Rev. Sci. Instrum.* 72:3956–3961.
17. So, P. T. C., T. Ragan, K. Bahlmann, H. Huang, K. H. Kim, et al. 2005. High-throughput tissue image cytometry. *In* Reviews in Fluorescence 2005. C. D. Geddes, and J. R. Lakowicz, editors. Springer, New York, pp. 325–347.
18. Ecker, R. C., and A. Tarnok. 2005. Cytomics goes 3D: toward tissomics. *Cytometry A.* 65:1–3.
19. Brandt, B. H., A. Roetger, T. Dittmar, G. Nikolai, M. Seeling, et al. 1999. c-erbB-2/ EGFR as dominant heterodimerization partners determine a motogenic phenotype in human breast cancer cells. *FASEB J.* 13:1939–1949.
20. Liu, J. T. C., M. J. Mandella, J. M. Crawford, C. H. Contag, G. S. Kino, et al. 2006. Performance of a dual-axes reflectance confocal microscope for imaging colonic neoplasia. *J. Biomed. Opt.* 11:054019.
21. Liu, J. T. C., M. J. Mandella, J. M. Crawford, C. H. Contag, T. D. Wang, et al. 2008. Efficient rejection of scattered light enables deep optical sectioning in turbid media with low-NA optics in a dual-axis confocal architecture. *J. Biomed. Opt.* 13:034020.